AIP | Applied Physics Letters

Damping properties for vibration suppression in electrohydraulic servo-valve torque motor using magnetic fluid

Jinghui Peng, Songjing Li, and Hasiaoqier Han

Citation: Applied Physics Letters **104**, 171905 (2014); doi: 10.1063/1.4875029
View online: http://dx.doi.org/10.1063/1.4875029
View Table of Contents: http://scitation.aip.org/content/aip/journal/apl/104/17?ver=pdfcov
Published by the AIP Publishing

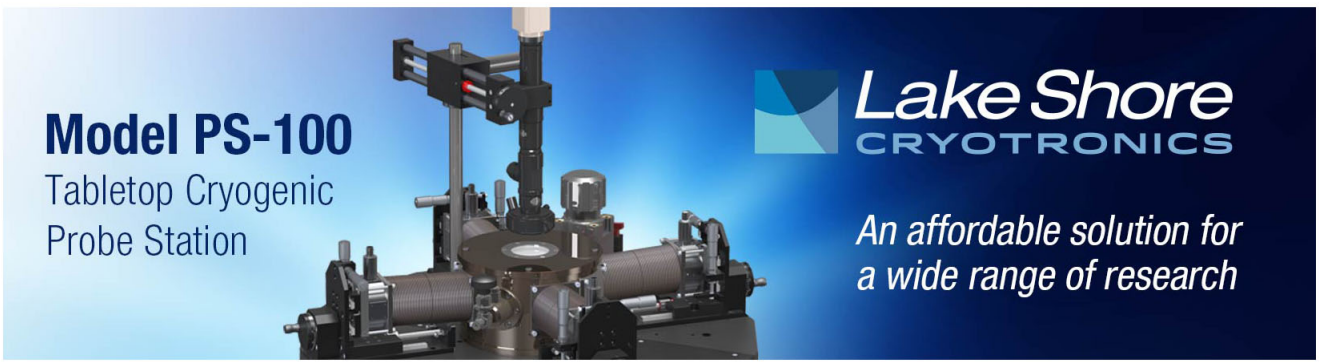

Damping properties for vibration suppression in electrohydraulic servo-valve torque motor using magnetic fluid

Jinghui Peng,[1] Songjing Li,[1,a)] and Hasiaoqier Han[2]
[1]*Department of Fluid Control and Automation, Harbin Institute of Technology, Harbin, Heilongjiang 150001, China*
[2]*Changchun Institute of Optics, Fine Mechanics and Physics, Chinese Academy of Sciences, Changchun, Jilin 130033, China*

(Received 12 March 2014; accepted 22 April 2014; published online 2 May 2014)

Aiming to suppress high frequency vibrations of a torque motor in electrohydraulic servo-valves, damping properties of an ester-based Fe_3O_4 magnetic fluid operating in the squeeze mode are studied in this Letter. The expression of damping forces due to the magnetic fluid on the torque motor is derived and simplified based on the measured magneto-viscosity property. Dynamic characteristics of the torque motor with and without the magnetic fluid are simulated and tested. Damping properties of magnetic fluid for the vibration suppression of a torque motor are verified by the good agreement between the predicted and tested results. © *2014 AIP Publishing LLC*.
[http://dx.doi.org/10.1063/1.4875029]

As a functional fluid material whose properties can be controlled by an external magnetic field, magnetic fluid (MF) has been getting more and more attention since the past decade. MF exhibits many remarkable properties and has been used in a wide variety of applications, such as applications in dampers, sealing, electric motors, photonic devices, and brakes.[1–4] Investigations[5,6] showed that higher saturation magnetization and larger viscosity will be introduced when MF was exposed to a magnetic field. The properties of MF, such as saturation magnetization, magneto-viscosity, magneto-optical effects, and thermal properties, were studied thoroughly.[7–11] However, the understanding of working mechanism and damping properties of MF is still far from clear.

Hydraulic servo-valve is the key component whose characteristics influence the performance of the hydraulic control system significantly. As the electro-mechanical signal converter in hydraulic servo-valves, the torque motor and pilot stage can deteriorate the characteristics or even cause the failure of servo-valves due to unpredictable self-excited pressure oscillations in the pilot flow field and armature vibrations at high frequencies.[12,13] Due to the magnetization characteristics of MF when exposed to a magnetic field, squeeze forces can be applied to the armature when MF is filled into the working gaps of the torque motor and operates in the squeeze mode, which makes MF an effective damper to depress the vibrations and improve the reliability of servo-valves.

The basic operational modes of MF devices were classified as: the direct shear mode, the valve mode, and the squeeze mode.[14,15] Being studied most extensively, especially in the mathematical modeling of MF basic properties, the shear and valve modes found more applications in MF devices than the squeeze mode.[16,17] For these two modes, Bingham-plastic and Herschel-Bulkley models are proved to be reasonable and applicable for the descriptions of the constitutive characteristics of MF because of the simplicity and efficiency. While for the squeeze mode, biviscosity model was suggested to be used for the theoretical analysis of MF behavior to avoid the "squeeze-flow paradox."[18–21] Yang theoretically analyzed the squeeze flow of the Bingham material in the small gap between two parallel disks based on a biviscosity constitutive model.[22] Ayadi presented exact analytic solutions for a squeeze flow of a Bingham fluid described by the biviscosity model.[23] However, the models are both complicated and far from applicable for the description of squeeze force.

In this Letter, the constitutive characteristics of MF are described using a biviscosity model. Based on the governing equations of fluid mechanics, the expression of damping forces due to the squeeze flow of MF on the torque motor is derived and linearized. The damping properties are validated through numerical simulation and experiment when MF is filled into the torque motor of a hydraulic servo-valve.

As shown in Fig. 1, MF in the working gaps of the torque motor operates in the squeeze mode when the armature

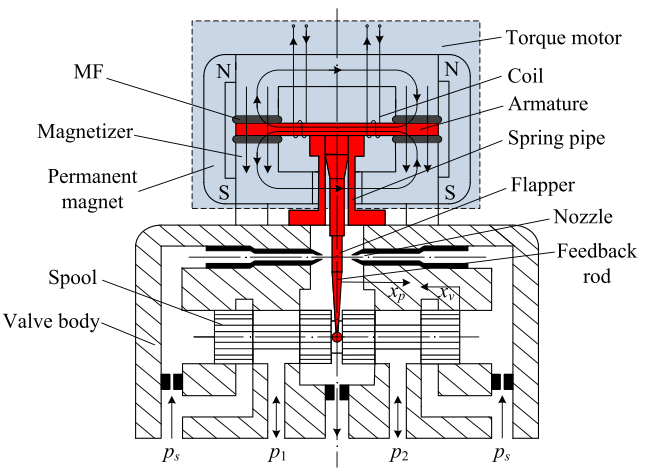

FIG. 1. Construction of a hydraulic servo-valve with MF. The hydraulic servo-valve consists of two parts, the torque motor and two-stage hydraulic amplifier. The pilot stage is a nozzle-flapper valve while the power stage is a spool valve.

[a)]Author to whom correspondence should be addressed. Electronic mail: lisongjing@hit.edu.cn

rotates. When the rotation angle is in a small range, the operational mode of MF can be equivalent to a symmetric extrusion, as shown in Fig. 2. For an ester-based Fe_3O_4 magnetic fluid, the generalized biviscosity model can be described as

$$\begin{cases} \tau_{yx} = \eta \dfrac{\partial u_x}{\partial y}, & |\tau_{yx}| < \tau_1 \\ \tau_{yx} = \operatorname{sgn}\left(\dfrac{\partial u_x}{\partial y}\right)\tau_0 + k\dfrac{\partial u_x}{\partial y}, & |\tau_{yx}| \geq \tau_1, \end{cases} \tag{1}$$

where τ_{xy} is the shear stress; τ_1 is the yield stress of MF; τ_0 is the dynamic yield stress varying with the applied magnetic field; μ_x is the velocity of MF in x direction; k and η are viscosities of MF in yield and non-yield region, respectively.

From Fig. 2, when $L \gg h$ and squeezing velocity is small, the squeeze flow of MF in the working gaps of torque motor can be assumed as incompressible steady flow. By combining mass and momentum conservation equations, the damping forces due to MF on the torque motor can be derived as

$$\begin{aligned} F = {} & \frac{2(\eta - k)W{\tau_1}^3h^3}{27\eta^3V^2} + \frac{2kVWL^3}{h^3} + \frac{3W\tau_0}{2h}\left(L^2 - \frac{{\tau_1}^2h^4}{9\eta^2V^2}\right) \\ & + 4LW\eta\left|\frac{-3kV{\tau_1}^2}{\eta h^3}\left(\frac{3kVL}{h^3} + \frac{3\tau_0}{2h}\right)^{-3} + \frac{3kV}{h^3}\left[\frac{1}{2k}(\tau_1 - \tau_0)^2 - \frac{{\tau_0}^2}{2k}\right]\left(\frac{3kVL}{h^3} + \frac{3\tau_0}{2h}\right)^{-2} + \frac{3V}{2h}\right|, \end{aligned} \tag{2}$$

where W is the width of the working gap.

From the above equation, it can be concluded that some parameters (such as τ_0, τ_1, η, and k) are crucial for the calculation of the damping forces. Because these parameters are influenced greatly by the concentration of MF and magnetic field, the viscosity of applied MF is measured with a viscometer (RVDV-II + Pro, Brookfield Company, MA, United States) to obtain the magneto-viscosity property of MF in this work. Figure 3 shows the schematic diagram of the viscometer. The value of viscosity can be determined by[24,25]

$$\eta = K\frac{M}{\omega}, \tag{3}$$

where K is relevant with the geometrical parameters of experimental setup, M and ω are drive torque and angular velocity of the rotor.

The shear stress at radius r can be calculated as[26]

$$\tau = \eta\dot{\gamma}, \tag{4}$$

where $\dot{\gamma}$ is the shear rate at radius r and $\dot{\gamma} = -r\frac{d\omega}{dr}$.

Figure 4 shows the measured shear stress of MF as a function of shear rate in different magnetic induction intensity. From the results in Fig. 4, it can be concluded that the shear stress of applied MF increases with the shear rate linearly for a given magnetic induction intensity. Additionally, the higher the magnetic induction intensity, the higher the shear stress, at the same shear rate. From Fig. 4, we can also get the relationship between dynamic yield stress and magnetic induction intensity, as shown in Fig. 5. Figure 5 shows that dynamic yield stress increases with magnetic induction intensity and tends to saturate in higher intensities. The saturation magnetic induction intensity for MF used in this work is about 450 GS.

The measured magnetic induction intension in the working gaps of torque motor varies from 2100 GS to 2500 GS during the working process of torque motor. A gauss meter

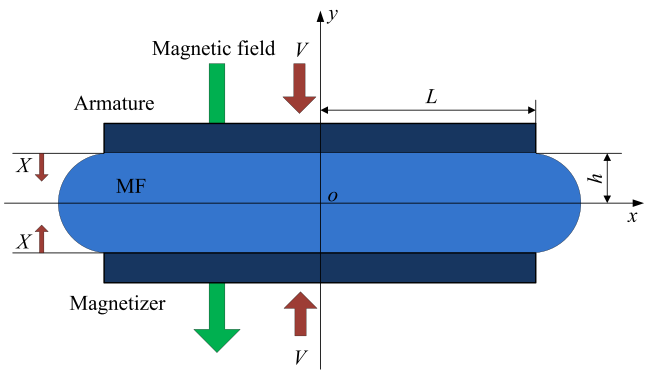

FIG. 2. Schematic diagram of squeeze mode for MF in the working gap. The squeeze mode is equivalent to symmetric extrusion. X and V are half the displacement and velocity of the armature. L and h are half the length and height of the working gap.

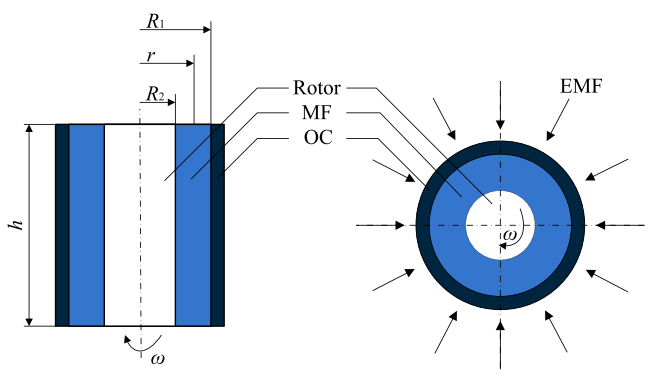

FIG. 3. Schematic diagram of the viscometer: Rotor, rotates with an angular velocity ω; MF, ester-based Fe_3O_4 magnetic fluid; OC, outer cylinder, used to contain MF; EMF, external magnetic field, perpendicular to shear velocity.

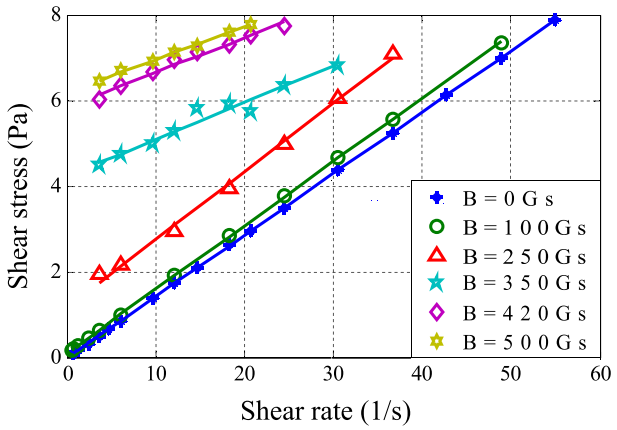

FIG. 4. Experimental results of shear stress vs shear rate under six different magnetic induction intensities for ester-based Fe_3O_4 MF.

(TX-15, Ch-Hall Co., Ltd., Beijing, China) is utilized for the measurement. Therefore, MF filled in the working gaps always gets saturated. Based on the experimental data (B = 500 GS) in Fig. 4, the magneto-viscosity property parameters (τ_0, τ_1, η, and k) under saturated state can be obtained and the damping forces due to MF on the armature of the torque motor can be calculated. In this work, the tested maximum displacement of armature is 76.9 μm and maximum velocity is 0.54 m/s, after MF is applied. The simulation results of damping forces due to MF are shown in Fig. 6.

Figure 6 shows the numerical results of damping forces varying with the squeezing displacement under six different squeezing velocities for ester-based Fe_3O_4 MF. From Fig. 6, it can be seen that the damping force increases with the squeezing displacement and velocity linearly. Therefore, the mathematical model for the damping force due to MF can be simplified and linearized as

$$F = K_c \times X + B_c \times V, \tag{5}$$

where K_c and B_c are the equivalent stiffness and damping coefficient which are the functions of squeezing displacement and velocity.

The simplified equation shows that the function of MF to the torque motor can be taken as the combinational working of a linear spring and viscosity damper when the squeezing displacement and velocity are in a small range.

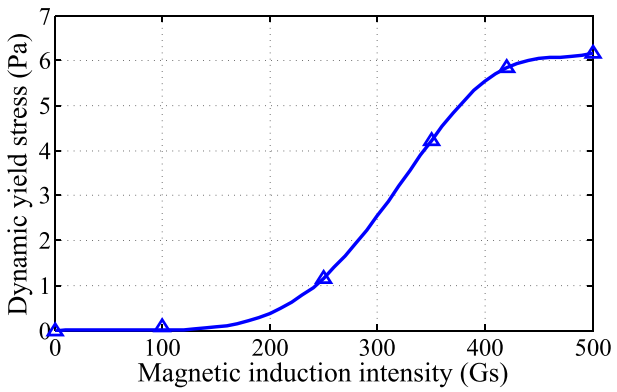

FIG. 5. Dynamic yield stress vs magnetic induction intensity. The dynamic yield stress is the shear stress developed in response to zero shear rate.

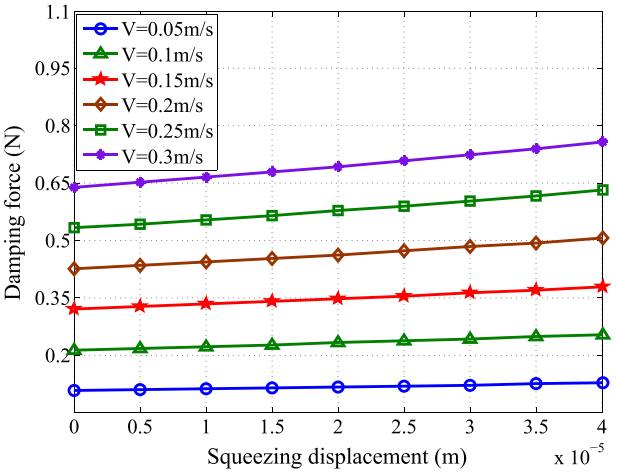

FIG. 6. Numerical results of damping force as a function of squeezing displacement under six different squeezing velocities for ester-based Fe_3O_4 MF.

Based on the simplified expression of damping forces, we numerically simulate the dynamic characteristics of the torque motor without any arbitrary loads to check the damping effect of MF on torque motor. In the simulation, MF is simulated using spring-damper elements, and K_c and B_c are mean values ($K_c = 200$ N/m, $B_c = 0.94$ N s/m) corresponding to the range of squeezing displacement and velocity of the armature. The dynamic amplitude responses are acquired by calculating the displacements at the end of the feedback rod. Numerical results of dynamic amplitude responses of the torque motor with and without MF are shown in Fig. 7. The results show that large resonance peaks occur at the natural frequencies when MF is not applied. That means a small damping ratio in the system without MF. Also large oscillations of the armature may happen during the transient process. When MF is applied on the torque motor, the resonance peaks are reduced obviously. It means large damping forces have been introduced due to MF. Figure 7 also shows that the natural frequencies of torque motor decrease slightly after MF is applied. That is because the total mass of the armature is increased by the application of MF.

To compare with the simulation results, dynamic characteristics of the torque motor with and without MF are tested. The schematic diagram of the experimental setup is

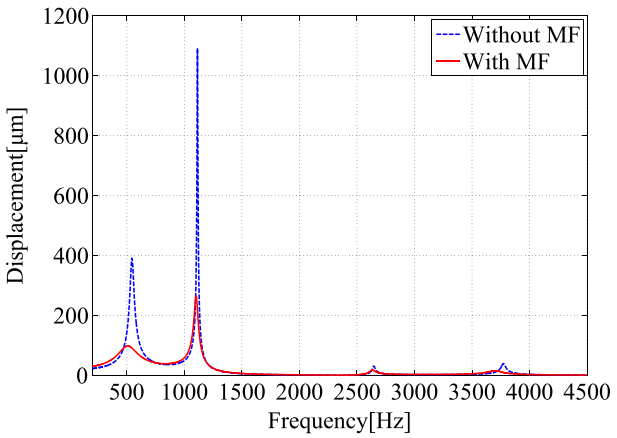

FIG. 7. Numerical results of dynamic amplitude responses of the torque motor with and without MF in frequency domain.

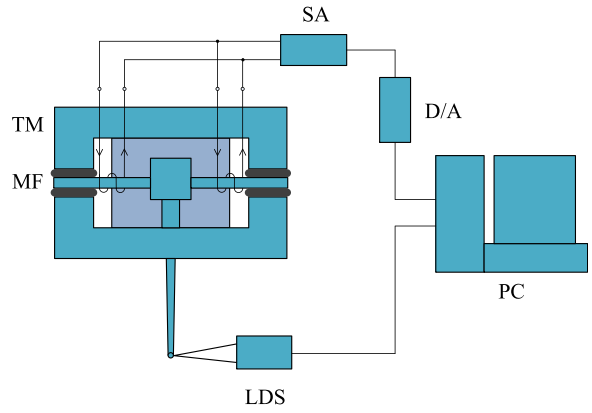

FIG. 8. Schematic diagram of dynamic experiment: TM, torque motor; MF, ester-based Fe_3O_4 magnetic fluid; LDS, laser displacement sensor; PC, personal computer; D/A, digital-analog converter; SA, servo amplifier.

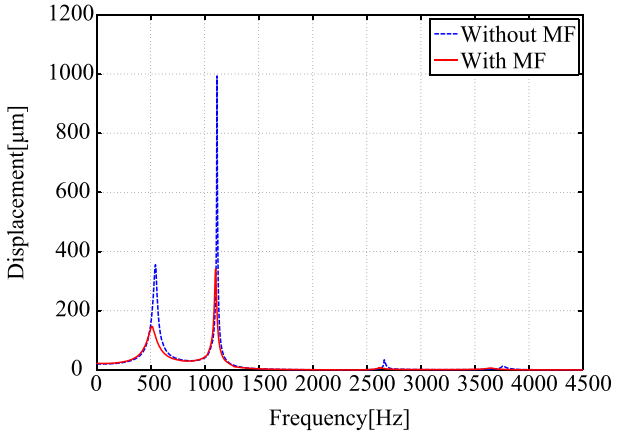

FIG. 9. Experimental results of dynamic amplitude responses of the torque motor with and without MF in frequency domain.

shown in Fig. 8. In the experiment, a number of sinusoidal current signals are supplied to the torque motor with frequency changed from 1 Hz to 4500 Hz and amplitude kept to be 10 mA. The dynamic amplitude responses of the torque motor are acquired by measuring the displacements at the end of the feedback rod using a laser displacement sensor (LK-G5000, Keyence Company, Osaka, Japan). The experimental results are shown in Fig. 9. It can be seen that the experimental results achieve a good agreement with the numerical ones. The resonance amplitudes are reduced significantly when MF is filled into the torque motor. The damping properties of MF for the vibration suppression of the torque motor are verified experimentally. Besides, the natural frequencies of the torque motor without MF are also larger than the ones with MF. The good agreement proves that the modeling approach for MF presented in this Letter is reasonable and applicable.

In conclusion, the damping properties of MF on the servo-valve torque motor are verified through numerical and experimental methods. Damping forces can be introduced on the torque motor due to the squeeze flow of MF. At the limiting case when the squeezing displacement and velocity are in a small range, the function of MF can be seen as the combination of a linear spring and damper. Resonance amplitudes of the torque motor can be reduced significantly after MF is applied. By selecting proper kind of MF, the oscillations and noise in the servo-valve may be removed completely.

This research was financially supported by the National Natural Science Foundation of China (Project No. 50875055).

[1]K. Shimada, S. Shuchi, A. Shibayama, S. Kamiyama, and A. Satoh, Fluid Dyn. Res. **34**(1), 21 (2004).
[2]E. Uhlmann, G. Spur, N. Bayat, and R. Patzwald, J. Magn. Magn. Mater. **252**(1), 336 (2002).
[3]V. Polevikov and L. Tobiska, J. Magn. Magn. Mater. **289**, 379 (2005).
[4]A. Nethe, T. Scholz, H. D. Stahlmann, and M. Filtz, IEEE Trans. Magn. **38**(2), 1177 (2002).
[5]Q. Li, Y. M. Xuan, and J. Wang, Exp. Therm. Fluid Sci. **30**(2), 109 (2005).
[6]S. Rhodes, X. W. He, S. Elborai, S. H. Lee, and M. Zahn, J. Electrost. **64**(7–9), 513 (2006).
[7]A. Tămaş, Z. Gropşian, and R. Minea, Stud. Univ. Babes-Bolyai Chem. **54**(1), 143 (2009).
[8]W. H. Li, G. Chen, and S. H. Yeo, Smart Mater. Struct. **8**(4), 460 (1999).
[9]S. Odinaev, K. Komilov, and A. Zaripov, Russ. J. Phys. Chem. A **84**(7), 1242 (2010).
[10]Z. Y. Di, X. F. Chen, S. L. Pu, and Y. X. Xia, Appl. Phys. Lett. **89**(21), 211106 (2006).
[11]L. M. Perez, J. Bragard, D. Laroze, J. Martinez-Mardones, and H. Pleiner, J. Magn. Magn. Mater. **323**(6), 691 (2011).
[12]A. Misra, K. Behdinan, and W. L. Cleghorn, J. Fluids Struct. **16**(5), 649 (2002).
[13]A. Glaun, Power **156**(2), 80 (2012).
[14]J. D. Carlson and M. R. Jolly, Mechatronics **10**(4), 555 (2000).
[15]P. Kulkarni, C. Ciocanel, S. L. Vieira, and N. Naganathan, J. Intell. Mater. Syst. Struct. **14**(2), 99 (2003).
[16]A. Farjoud, R. Cavey, M. Ahmadian, and M. Craft, Smart Mater. Struct. **18**(9), 095001 (2009).
[17]A. G. Olabi and A. Grunwald, Mater. Des. **28**(10), 2658 (2007).
[18]S. D. R. Wilson, J. Non-Newton. Fluid Mech. **47**, 211 (1993).
[19]D. K. Gartling and N. Phan-Thien, J. Non-Newtonian Fluid Mech. **14**, 347 (1984).
[20]F. Imaduddin, S. A. Mazlan, and H. Zamzuri, Mater. Des. **51**, 575 (2013).
[21]D. H. Wang and W. H. Liao, Smart Mater. Struct. **20**(2), 023001 (2011).
[22]S. P. Yang and K. Q. Zhu, J. Non-Newtonian Fluid Mech. **138**(2), 173 (2006).
[23]A. Ayadi, J. Non-Newtonian Fluid Mech. **166**(21), 1253 (2011).
[24]H. G. Lee and S. B. Choi, Mater. Des. **23**(1), 69 (2002).
[25]K. Shimada, H. Nishida, and T. Fujita, Int. J. Mod. Phys. **15**(6), 1050 (2001).
[26]F. Omidbeygi and S. H. Hashemabadi, J. Magn. Magn. Mater. **324**(13), 2062 (2012).